Supporting Information

Mixed Protonic-Electronic Conducting Cathode with Ru Nanoparticles Catalyst for Electrochemical Ammonia Synthesis Based on a Proton-Conducting BZCYYb Electrolyte

*Jiaqi Chen[a,b], Wenbo Gao[*b,c], Liangzhu Zhu[d], Haoliang Tao[d], Sheng Feng[b], Hujun Cao[b,c], Jianping Guo[b,c], Yanxia Chen[*a], Ping Chen[b,]*

a. Hefei National Research Center for Physical Sciences at the Microscale, Department of Chemical Physics, University of Science and Technology of China, Hefei 230026, China,

b. Dalian Institute of Chemical Physics, Chinese Academy of Sciences, Dalian 116023, P. R. China,

c. Center of Materials Science and Optoelectronics Engineering, University of Chinese Academy of Sciences, Beijing 100049, P. R. China,

d. Ningbo Institute of Material Technology and Engineering, Chinese Academy of Science, Ningbo 315200, PR China.

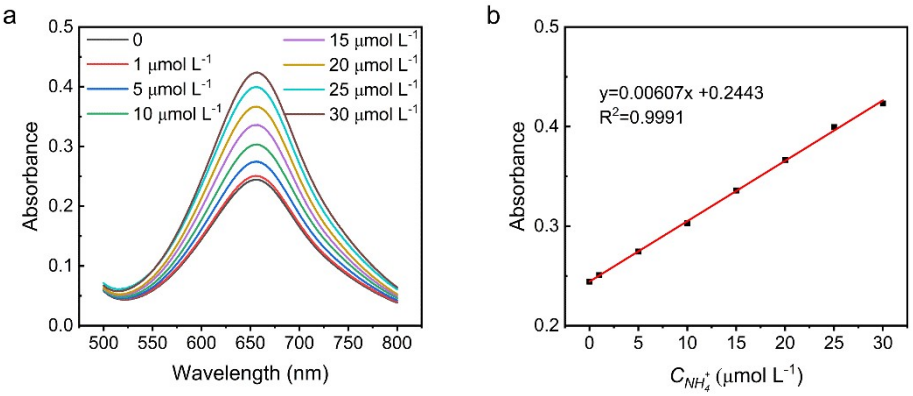

Figure S1 (a) UV-vis spectra obtained using standard solutions of NH_4Cl, (b) dependency of Abs on C_{NH4+}.

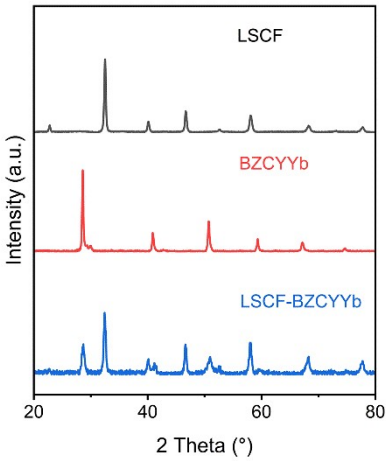

Figure S2 XRD patterns of the LSCF, the BZCYYb, and the LSCF-BZCYYb after sintering at 1100 ˚C.

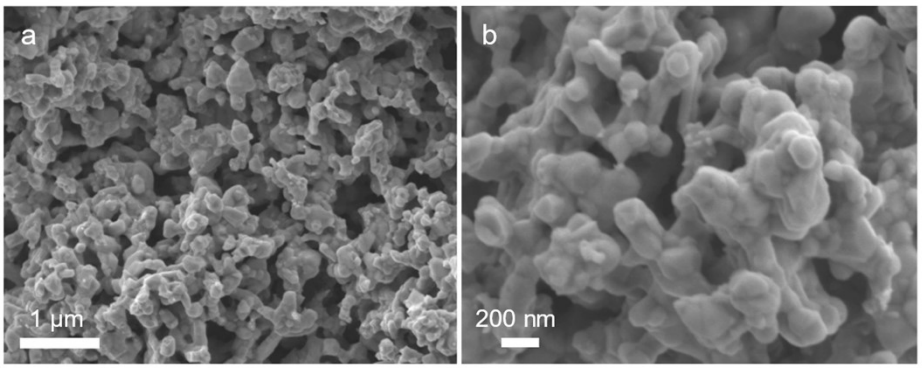

Figure S3 SEM images of the LSCF-BZCYYb cathode.

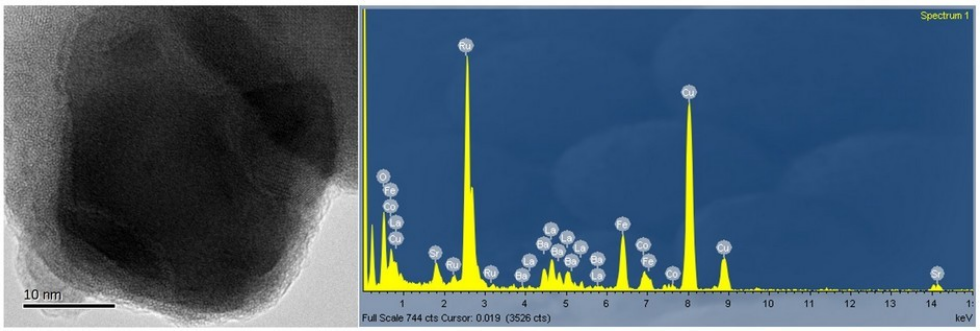

Figure S4 HR-TEM image and EDS of the I-Ru-LSCF-BZCYYb cathode.

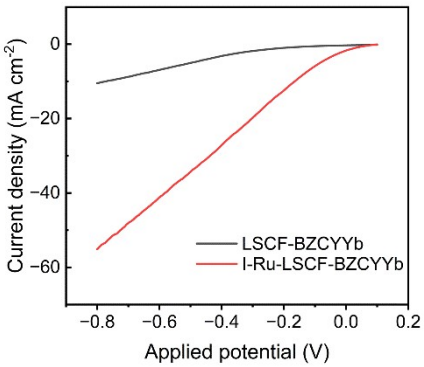

Figure S5 *j-E* curves of the LSCF-BZCYYb|BZCYYb|Ni-BZCYYb electrolysis cell and the I-Ru-LSCF-BZCYYb|BZCYYb|Ni-BZCYYb electrolysis cell, with a scan rate of 10 mV s^{-1}, at 400 ˚C. Reaction gas: pure N_2 at the working electrode; 5% H_2-95% Ar at the counter electrode (reference electrode).

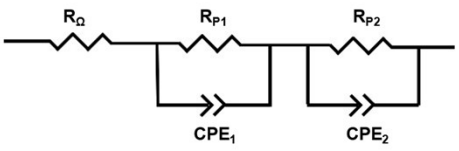

Figure S6 Equivalent circuit of PCEAS electrolysis cell.

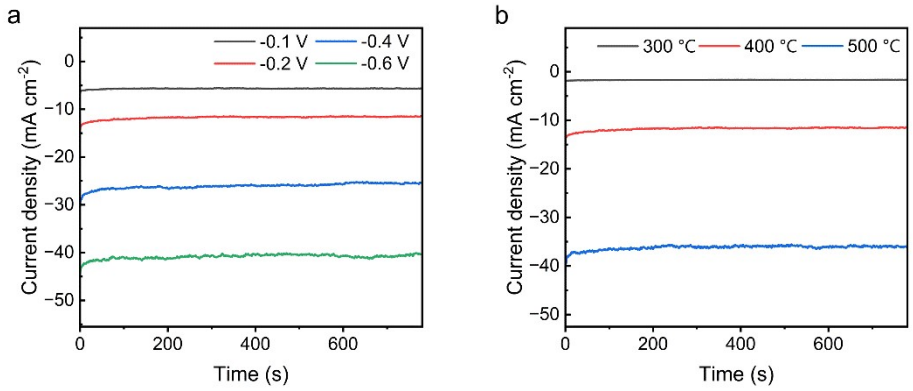

Figure S7 *j-t* curves of the I-Ru-LSCF-BZCYYb|BZCYYb|Ni-BZCYYb electrolysis cells, (a) at 400 °C and different potential, (b) at different temperatures and an applied potential of −0.2 V. Reaction gas: pure N_2 at the working electrode; 5% H_2-95% Ar at the counter electrode (reference electrode).

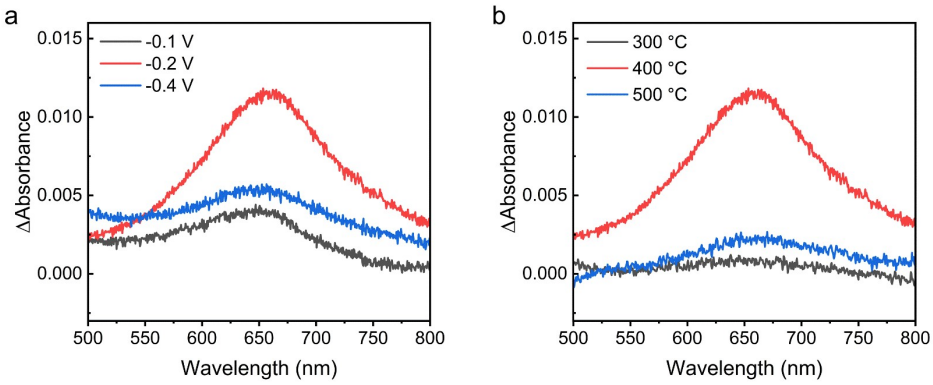

Figure S8 The differential UV-vis spectra (calibrated with blank solution) of the solutions which absorbed the outlet gas from the I-Ru-LSCF-BZCYYb|BZCYYb|Ni-BZCYYb electrolysis cell, (a) at 400 °C and different potential, (b) at different temperatures and an applied potential of −0.2 V. Reaction gas: pure N_2 at the working electrode; 5% H_2-95% Ar at the counter electrode (reference electrode).

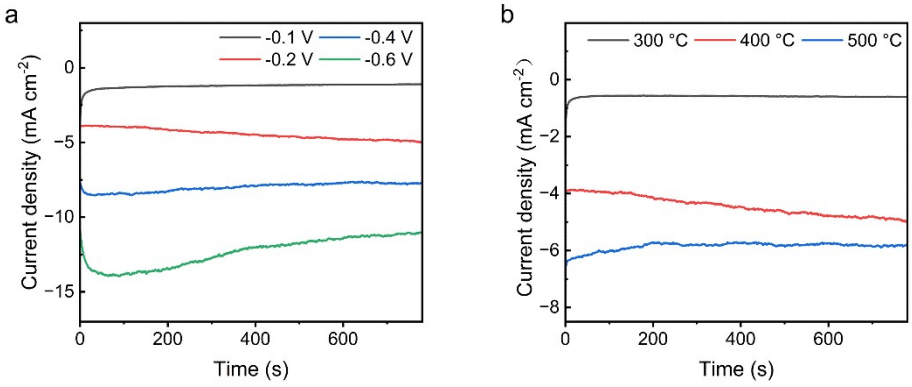

Figure S9 *j-t* curves of the I-Ru-BZCYYb|BZCYYb|Ni-BZCYYb electrolysis cells, (a) at 400 °C and different potential, (b) at different temperatures and an applied potential of −0.2 V. Reaction gas: pure N_2 at the working electrode; 5% H_2-95% Ar at the counter electrode (reference electrode).

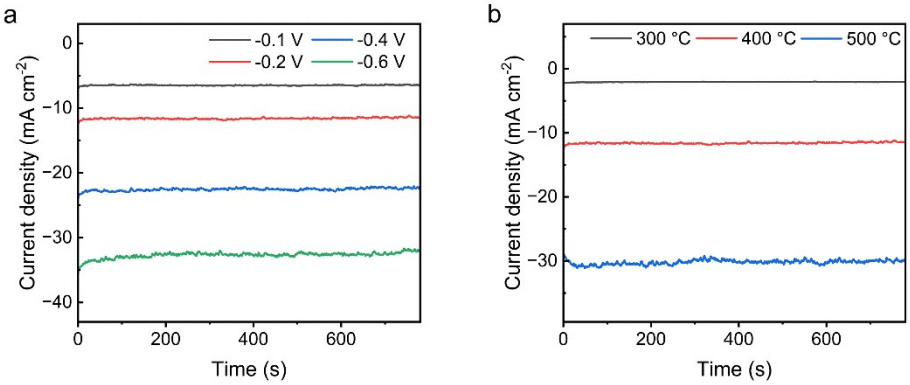

Figure S10 *j-t* curves of the M-Ru-LSCF-BZCYYb|BZCYYb|Ni-BZCYYb electrolysis cells, (a) at 400 °C and different potential, (b) at different temperatures and an applied potential of −0.2 V. Reaction gas: pure N_2 at the working electrode; 5% H_2-95% Ar at the counter electrode (reference electrode).

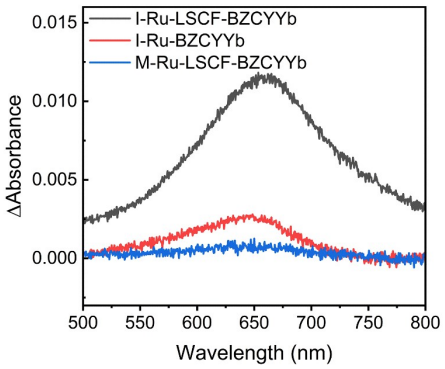

Figure S11 The differential UV-vis spectra (calibrated with blank solution) of the solutions which absorbed the outlet gas from the I-Ru-LSCF-BZCYYb|BZCYYb|Ni-BZCYYb, the M-Ru-LSCF-BZCYYb|BZCYYb|Ni-BZCYYb, and the I-Ru-BZCYYb|BZCYYb|Ni-BZCYYb electrolysis cells at the optimum condition. Reaction gas: pure N_2 at the working electrode; 5% H_2-95% Ar at the counter electrode (reference electrode).

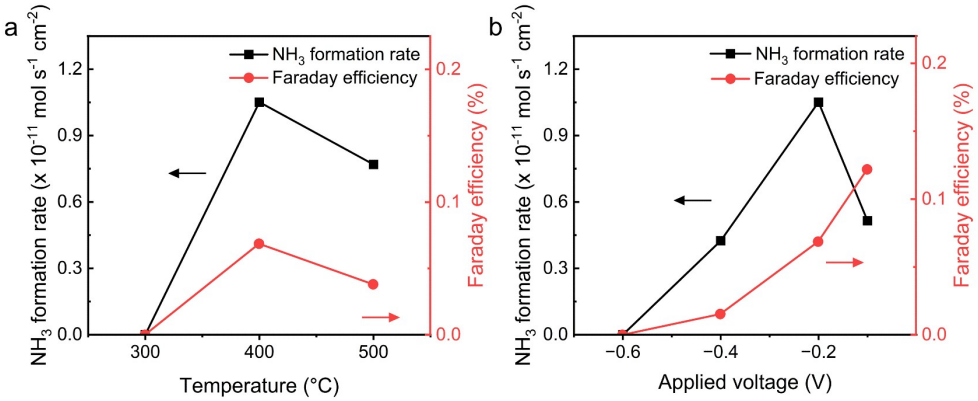

Figure S12 NH_3 formation rate and faraday efficiency of the I-Ru-BZCYYb|BZCYYb|Ni-BZCYYb electrolysis cell (a) at different temperature and an applied potential of −0.2 V, (b) at 400 ˚C and different voltage. Reaction gas: pure N_2 at the working electrode; 5% H_2-95% Ar at the counter electrode (reference electrode).

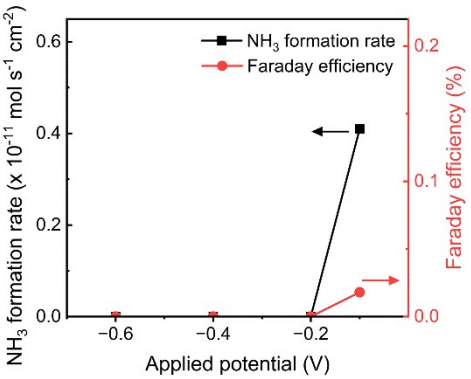

Figure S13 NH_3 formation rate and faraday efficiency of the M-Ru-LSCF-BZCYYb|BZCYYb|Ni-BZCYYb electrolysis cell at 400 ˚C and different potential. Reaction gas: pure N_2 at the working electrode; 5% H_2-95% Ar at the counter electrode (reference electrode).

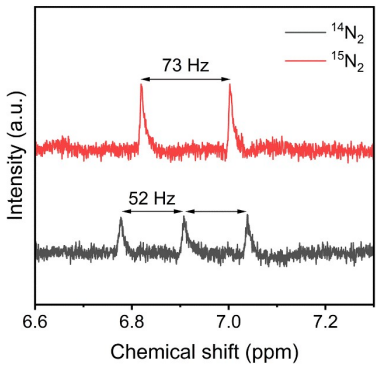

Figure S14 ^1H NMR spectra of the solutions which absorbed the outlet gas from the I-Ru-LSCF-BZCYYb|BZCYYb|Ni-BZCYYb electrolysis cell operating at −0.2 V and 400 ˚C using $^{15}N_2$ or $^{14}N_2$ as reaction gas, respectively.

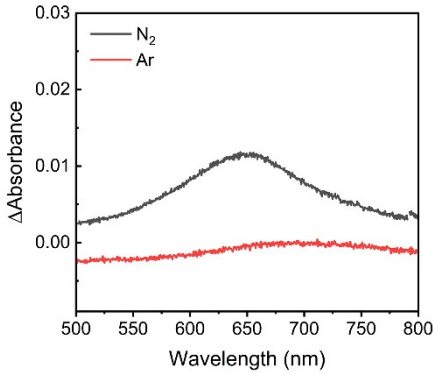

Figure S15 The differential UV-vis spectra (calibrated with blank solution) of the solutions which absorbed the outlet gas from the I-Ru-LSCF-BZCYYb|BZCYYb|Ni-BZCYYb electrolysis cell operating at −0.2 V and 400 ˚C. Reaction gas: pure N_2 or Ar at the working electrode; 5% H_2-95% Ar at the counter electrode (reference electrode).

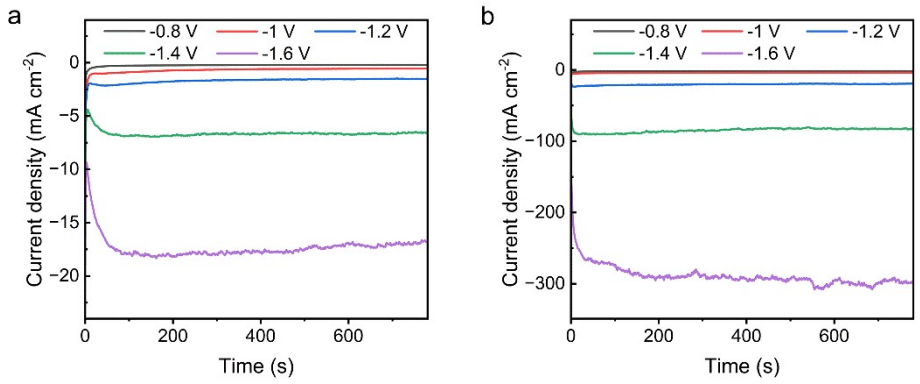

Figure S16 *j-t* curves of the I-Ru-LSCF-BZCYYb|BZCYYb|Ni-BZCYYb electrolysis cells, (a) at 400 °C and different potential, (b) at 500 °C and different potential. Reaction gas: pure N_2 at the working electrode; wet Ar at the counter electrode (reference electrode).

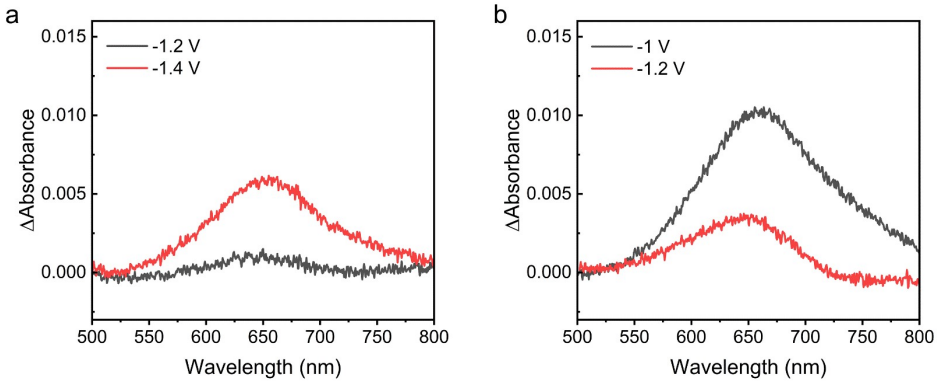

Figure S17 The differential UV-vis spectra (calibrated with blank solution) of the solutions which absorbed the outlet gas from the I-Ru-LSCF-BZCYYb|BZCYYb|Ni-BZCYYb electrolysis cells, (a) at 400 °C and different potential, (b) at 500 °C and different potential. Reaction gas: pure N_2 at the working electrode; wet Ar at the counter electrode (reference electrode).

Table S1 Increase in absorbance at 655 nm of UV-vis spectrogram of the solutions which absorbed the outlet gas from electrolysis cells with different cathodes operating at 400 °C and different potential. Reaction gas: pure N_2 at the working electrode; 5% H_2-95% Ar at the counter electrode (reference electrode).

Cathode	−0.1 V	−0.2 V	−0.4 V	−0.6 V
I-Ru-LSCF-BZCYYb	0.0039	0.0114	0.0053	-
I-Ru-BZCYYb	0.0011	0.0023	0.0009	-
M-Ru-LSCF-BZCYYb	0.0009	-	-	-

"—" indicates that the change in absorbance is close to 0. The amount of ammonia produced can be calculated through the formula: n=6×△Abs/6.07; (6 mL is the volume of the absorbing solutionis; 6.07 is slope of standard curve)

Table S2 Increase in absorbance at 655 nm of UV-vis spectrogram of the solutions which absorbed the outlet gas from electrolysis cells with different cathodes operating at −0.2 V and different temperature. Reaction gas: pure N_2 at the working electrode; 5% H_2-95% Ar at the counter electrode (reference electrode).

Cathode	300 ˚C	400 ˚C	500 ˚C
I-Ru-LSCF-BZCYYb	0.0007	0.0114	0.0022
I-Ru-BZCYYb	-	0.0023	0.0017
M-Ru-LSCF-BZCYYb	-	-	-

Table S3 Total charge in the chronoamperometry of electrolysis cells with different cathodes operating at 400 °C and different potential. Reaction gas: pure N_2 at the working electrode; 5% H_2-95% Ar at the counter electrode (reference electrode).

Cathode	−0.1 V	−0.2 V	−0.4 V	−0.6 V
I-Ru-LSCF-BZCYYb	1.24 C	2.56 C	5.69 C	8.92 C
I-Ru-BZCYYb	0.27 C	0.97 C	1.75 C	2.70 C
M-Ru-LSCF-BZCYYb	1.41 C	2.53 C	4.92 C	7.14 C

Table S4 Total charge in the chronoamperometry of electrolysis cells with different cathodes operating at −0.2 V and different temperature. Reaction gas: pure N_2 at the working electrode; 5% H_2-95% Ar at the counter electrode (reference electrode).

Cathode	300 ˚C	400 ˚C	500 ˚C
I-Ru-LSCF-BZCYYb	0.37 C	2.56 C	7.88 C
I-Ru-BZCYYb	0.13 C	0.97 C	1.28 C
M-Ru-LSCF-BZCYYb	0.45 C	2.53 C	6.59 C

Table S5 Increase in absorbance at 655 nm of UV-vis spectrogram of the solutions which absorbed the outlet gas from the I-Ru-LSCF-BZCYYb|BZCYYb|Ni-BZCYYb electrolysis cell operating at different temperatures and potentials. Reaction gas: pure N_2 at the working electrode; wet Ar at the counter electrode (reference electrode).

Temperature	−0.8 V	−1 V	−1.2 V	−1.4 V	−1.6 V
400 ˚C	-	-	0.0008	0.0059	-
500 ˚C	-	0.0101	0.0035	-	-

Table S6 Total charge in the chronoamperometry of the I-Ru-LSCF-BZCYYb|BZCYYb|Ni-BZCYYb electrolysis cell operating at different temperatures and potentials. Reaction gas: pure N_2 at the working electrode; wet Ar at the counter electrode (reference electrode).

Temperature	−0.8 V	−1 V	−1.2 V	−1.4 V	−1.6 V
400 ˚C	0.05 C	0.15 C	0.37 C	1.45 C	3.79
500 ˚C	0.40 C	0.92 C	4.44 C	18.50 C	63.12